

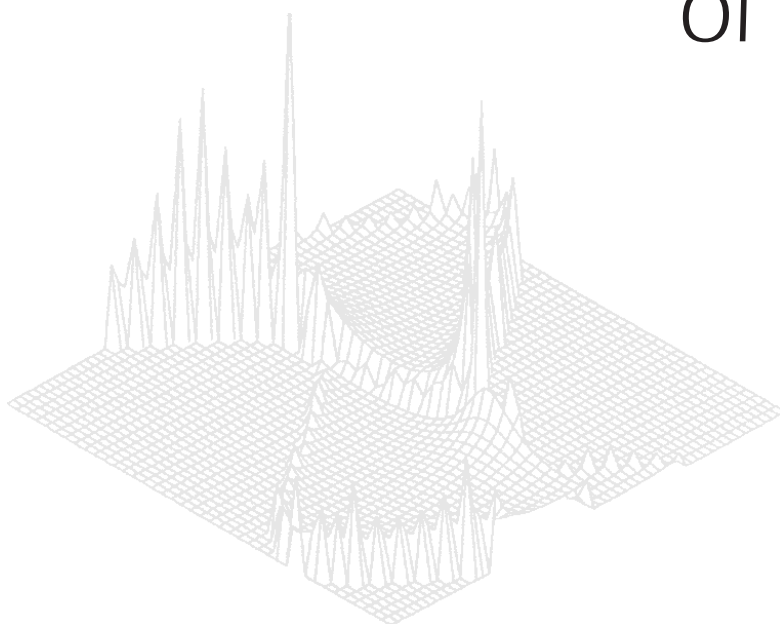
---

CSIRO PUBLISHING

---

# Australian Journal of Physics

Volume 53, 2000  
© CSIRO 2000



A journal for the publication of  
original research in all branches of physics

**[www.publish.csiro.au/journals/ajp](http://www.publish.csiro.au/journals/ajp)**

All enquiries and manuscripts should be directed to

*Australian Journal of Physics*

**CSIRO PUBLISHING**

PO Box 1139 (150 Oxford St)

Collingwood

Vic. 3066

Australia

Telephone: 61 3 9662 7626

Facsimile: 61 3 9662 7611

Email: [peter.robertson@publish.csiro.au](mailto:peter.robertson@publish.csiro.au)



Published by **CSIRO PUBLISHING**  
for CSIRO and  
the Australian Academy of Science



## Density Matrix Renormalisation Group Method and Symmetries of the Hamiltonian\*

Ian P. McCulloch and Miklos Gulácsi

Department of Theoretical Physics,  
Research School of Physical Sciences and Engineering,  
Australian National University,  
Canberra, ACT 0200, Australia.

### Abstract

Substantial improvements in the computational effort in a density matrix renormalisation program can be made by utilising symmetries of the Hamiltonian. Extra quantum numbers are always desirable to include in the calculation, since it allows the Hilbert space of the superblock to be refined. Since the speed of the calculation is approximately  $O(n^3)$  in superblock states, the speed increase in targeting a specific total spin state can be considerable. In this paper a new density matrix renormalisation algorithm is presented which conserves the total spin. The general procedure obtained works for any operator, even operators that do not commute with the Hamiltonian.

### 1. Introduction

The central problem posed by heavy fermion materials is to understand the interaction between an array of localised moments (generally f-electrons in lanthanide or actinide ions) and conduction electrons (generally p- or d-band). The magnetic properties of this localised moments and conduction electron interplay is well described by the Kondo lattice model:

$$H = -t \sum_{\langle i,j \rangle, \alpha} c_{i,\alpha}^\dagger c_{j,\alpha} + J \sum_j \mathbf{S}_{cj} \cdot \mathbf{S}_j, \quad (1)$$

where  $t \equiv 1$  is the conduction electron hopping,  $\langle i, j \rangle$  denotes nearest neighbours,  $\mathbf{S}_j$  are spin 1/2 operators for the localised spins, and where  $\mathbf{S}_{cj} = \frac{1}{2} \sum_{\alpha, \alpha'} c_{j,\alpha}^\dagger \boldsymbol{\sigma}_{\alpha, \alpha'} c_{j,\alpha'}$  with  $\boldsymbol{\sigma}$  the Pauli spin matrices and  $c_{j,\alpha}, c_{j,\alpha}^\dagger$  the electron site operators.

For partially conduction electron band filling, i.e.  $n = N_c/L < 1$ , where  $N_c$  is the number of electrons and  $L$  the number of localised spins of the one-dimensional chain, the physics of the Kondo lattice model is dominated by ferromagnetism (Honner and Gulácsi 1997a, 1998a). The conduction electrons couple together the impurity spins (Honner and Gulácsi 1997b, 1998b) in a mechanism analogous to double-exchange (Honner and Gulácsi 1997c). This ferromagnetic phase has been previously seen in numerical simulations by a variety of methods (Troyer and Würtz 1993; Tsunetsugu *et al.* 1993; Moukouri and Caron 1995) for values of the conduction electron filling factors less than quarter filling. The true paramagnetic–ferromagnetic phase boundary was first identified analytically (Honner

\* Refereed paper based on a contribution to the Ninth Gordon Godfrey Workshop on Condensed Matter in Zero, One and Two Dimensions held at the University of New South Wales, Sydney, in November 1999.

and Gulácsi 1997*a*, 1998*a*) using a new bosonisation method which allows electrons to overlap. The calculation has been confirmed by the density matrix renormalisation group (DMRG) by Caprara and Rosengren (1997*a*) for less than quarter filling and more recently by McCulloch *et al.* (1999) for regions above a quarter filling.

Previous failures to detect the ferromagnetic phase boundaries for any  $n$  using the DMRG can be attributed to the fact that the existing numerical packages do not keep track of the total spin or magnetisation, which is a crucial criterion in determining the ferromagnetism. By neglecting these parameters, the previous DMRG methods could not reveal the full complexity of the model. Thus we modified the standard DMRG algorithm to explicitly include the total spin quantum number. This greatly facilitates calculations involving the ferromagnetic phase and determines the phase diagram even for  $n$  values very close to half filling (McCulloch *et al.* 1999). In this paper we present an overview of the DMRG with total spin and discuss the advantages and disadvantages of the method.

## 2. Why DMRG?

The original DMRG algorithm (White 1992, 1993) was developed to overcome the problems that arise in one-dimensional interacting systems when standard renormalisation group procedures are applied. The starting point for all the DMRG and renormalisation group calculations is a block Hamiltonian  $H_A$ , with some given set of boundary conditions. The traditional renormalisation group method follows closely the Kadanoff real space scaling ideas (Gulácsi and Gulácsi 1998), whereby two or more of such blocks are joined to create a superblock  $H_{AA'A''\dots}$  with a basis that is a direct product of the basis states of each individual block. This new Hamiltonian is diagonalised and only the lowest, e.g.  $m$ , eigenstates are kept. With these  $m$  eigenstates we form a new block  $H_B$  and the iteration is continued by forming a new superblock,  $H_{BB'B''\dots}$ , whose lowest  $m$  eigenvalues are kept, etc.

This method was extremely successful in certain cases (Wilson 1975; Krishna-murthy *et al.* 1980). However, it proved to be a very poor approximation to one-dimensional interacting electron systems (Bray and Chui 1987). In these systems, long range correlations and collective effects are paramount in describing the properties of the system. In the traditional renormalisation group technique these collective effects are suppressed because of the boundary conditions that apply to each block. If open boundary conditions are used, then eigenstates of  $H_A$  will have the wavefunction going to zero at the edges of the block. Thus, when the blocks are joined and the old block edges become adjacent and in the middle of the lattice, the resulting basis is not good at representing collective effects that span the whole system. A similar argument applies in the case of periodic boundary conditions. With the current understanding of one-dimensional systems and knowing how different these systems are from their three-dimensional counterparts it seems almost obvious that such an 'old fashioned' scheme will not work.

An electron sea in one dimension has particular characteristics which place it outside the Fermi liquid framework. The important properties are the following (Voit 1995; Gulácsi 1997): (1) The low-energy excitations of the one-dimensional electron sea are collective and exhibit a phenomena called spin and charge separation. This contradicts the three-dimensional picture in which the excitations resemble individual electron excitations. (2) The collective excitations do not interact at low energies, and one-dimensional systems with simple forward scattering interactions have a universal structure composed of independent harmonic oscillators. (3) As a consequence of (2), the momentum

distribution is continuous—in the one-dimensional electron sea the spectral weight  $Z$  vanishes and the system does not support low-energy quasi-particle excitations.

The theory of the one-dimensional electron sea was pioneered by Haldane (Voit 1995; Gulácsi 1997) and has been developed since by numerous theoretical physicists over the years and is known as the ‘Luttinger liquid’ theory. In this theory the destruction of quasi-particles and the fact that  $Z = 0$  is due to the non-zero momentum transfer processes. It is possible to go beyond perturbation theory and, consistent with  $Z = 0$ , one indeed finds that the elementary excitations at low energy are collective bosonic charge and spin fluctuations. The origin of this so-called ‘spin and charge separation’ can be described in a number of ways, all of which refer to the nature of the one-dimensional phase space. The one-dimensional Fermi surface consists of only two (traditionally called ‘left’ and ‘right’) points. Scattering processes which take place on the same Fermi point give rise to spin and charge separation. This phenomenon is seen in all one-dimensional electron systems and it seems that it is not related to other characteristics of one-dimensional systems, namely the renormalised correlation function exponents (the  $Z = 0$  effect mentioned earlier).

Accordingly, the main property of one-dimensional conductors is that their low lying excited states are charge and spin collective density modes. Due to these density modes the traditional numerical renormalisation group methods break down. This problem was recognised first by White (1992, 1993) who introduced the central idea of the DMRG, namely to keep the ‘most probable’ states of a smaller section of the lattice in such a way that additional lattice sites can be added without undesirable effects arising from the external boundary conditions. This idea follows from the requirement that for a collective density mode to be operational it must have the largest possible overlap between the blocks, i.e. it must have the largest eigenvalues of the corresponding block density matrix.

### 3. The DMRG Method

The way to achieve this is to split the complete system (‘superblock’) into two parts: one called the ‘system’ and the other the ‘environment’. At the first step of the calculation, each block typically comprises two complete sites. Let us assume that the system block basis is defined by a set of orthonormal states  $|i\rangle$ , for  $i = 1, 2, \dots, m$  and the environment by another set  $|j\rangle$ , for  $j = 1, 2, \dots, n$ . Then an arbitrary state including the system and its environment can be expressed as

$$|\Psi\rangle = \sum_{i,j} \psi_{i,j} |i\rangle |j\rangle. \quad (2)$$

Projecting onto the system block, the probability of a given system block state is determined by its weight in the superblock wavefunction:

$$W(|x\rangle) = \sum_{i,i',j} \langle x | \psi_{i,j} | i \rangle \langle i' | \psi_{i',j}^* | x \rangle. \quad (3)$$

This is easily expressed in terms of the *reduced density matrix* operator,

$$\rho = \sum_{i,i',j} \psi_{i,j} \psi_{i',j}^* |i\rangle \langle i'|. \quad (4)$$

The system block states with maximum probability can therefore be obtained by maximising equation (3), subject to the condition  $\langle x | x \rangle = 1$ , by using a Lagrange multiplier. This simple calculation leads to the result that the states of maximum probability are of the form

$$|x\rangle = \lambda \rho |x\rangle, \quad (5)$$

that is, the eigenstates of the reduced density matrix operator. Thus a good approximation to the Hilbert space can be made by taking the  $m$  eigenstates of the density matrix with highest eigenvalue. The ‘truncation error’ incurred by doing this can be calculated from the sum of the remaining eigenvalues. Typically, this is less than  $10^{-4}$  in a DMRG calculation. We can now add new sites (usually only one) to the system block, to form a product basis of size  $mq$ , where  $q$  is the number of single site basis states, and repeat the process thereby increasing the size of the system block by a fixed number of sites at each step.

This concept of the reduced density matrix forms the basic idea of the DMRG scheme (White 1992, 1993). The states selected to construct the new blocks are the eigenstates of the reduced matrix with the largest eigenvalues, since they represent the highest probability of a system under a given environment. It is clear that the scheme has nothing in common with the old-fashioned real space renormalisation group approaches and hence it is a historical accident that we still refer to it as a ‘renormalisation group’ method.

It is useful to label the block basis states by the conserved quantum numbers of the system. This means that a particular sector of the superblock Hilbert space (e.g. the subspace of some fixed number of electrons and  $z$ -component of spin) can be targeted. Importantly, this reduces the size of the superblock Hilbert space, as calculating the ground state wavefunction takes a time proportional to the cube of the number of basis states. Near degeneracies in the ground state can be handled much more easily if the states are in two different sectors of the Hilbert space. Instead of trying to keep enough states so that the expectation value of the operator can be calculated with enough accuracy, it is a relatively easy procedure to diagonalise separately each sector of the Hilbert space and calculate the energy gap. The particle number and  $z$ -component of the spin operators are the usual quantum numbers used in the DMRG, since these operators commute with the reduced density matrix. Thus the reduced density matrix is block diagonal with respect to the quantum numbers and it is relatively easy to keep track of the block basis states. However, for some conserved quantities, for example the total spin  $S^2$ , the corresponding operator does *not* commute with the reduced density matrix. This introduces additional complications which we address in a later section.

#### 4. The Algorithm

The simplest implementation of the DMRG method is to use the so-called ‘infinite size’ algorithm. In this algorithm, new sites are added to the system repeatedly, until the properties of the ground state converge, hopefully to something close to the true thermodynamic limit. Schematically, sites are added to the system and environment blocks as shown in Fig. 1. For systems with reflection symmetry, the environment block can simply be the spatial reflection of the system block. Thus the system grows by two lattice sites at each step. It is important to add an extra site to the environment block also, because of an important theorem: The number of non-zero eigenvalues of the density matrix is at most  $\min(m_{\text{system}}, m_{\text{environment}})$ , thus if we are keeping  $m$  system block states at the truncation,

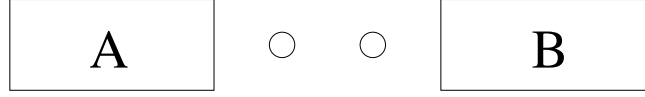


**Fig. 1.** One site is added to the system block  $A$  block and the environment block  $B$  at each step.

then we must have more than  $m$  states in the environment block. This theorem does not hold if more than one superblock state is used to construct the density matrix. In this case, it is possible to construct a useful algorithm where only one site is added at a time (White and Scalapino 1997, 1998).

The more common algorithm is the ‘finite size’ algorithm. In this scheme, the system is grown to a predetermined fixed size  $L$  using the infinite size method, at which point the system and environment blocks are each of size  $L/2$ . From here on, progressively smaller environment blocks are used such that the overall system size is a constant, e.g. at the next step, the system block would be  $L/2 + 1$  sites, and the environment block would be the old system block of size  $L/2 - 2$  plus one new site, thus preserving the overall length. Once the environment block gets down to just two lattice sites, the sweep can start again from a system block of  $2 + 1$  sites, and an environment block of  $(L - 4) + 1$  sites. Thus, many sweeps can be made over the superblock, improving the basis each time. The initial sweeps, where the basis is not expected to be very well converged anyway, can be made faster by keeping fewer states. A useful optimisation can be achieved by using the wavefunction from the previous step as the starting vector for finding the new ground state.

The computational advantage of the infinite size scheme is that there is very little storage requirement: at each iteration, the matrices used at the previous iteration can be discarded. For the finite size scheme, it is necessary to store the blocks for all lattice sizes.

It may seem that the above scheme is complicated, but it is not. The success of the DMRG relies on its simplicity and the fact that it can be easily implemented for any one-dimensional model. The required CPU time will depend on the how a long chain are we interested in and how many states are kept. The CPU time increases linearly with the length of the chain, although the cumulative truncation error also increases linearly.

## 5. Convergence

Even though the DMRG is widely used and has had spectacular successes in calculating ground state energies and many other properties of one-dimensional quantum systems, it has its limitations. In the infinite system algorithm, described previously, the results can be viewed as a segment of an infinite system. That is, by increasing the lattice size, the calculated ground state energy should approach the true ground state energy of the infinite system. This convergence criterion is not always satisfied. For non-fermionic models such as spin chains or bosonic systems, and for fermionic models where the number of fermions is an exact multiple of the number of lattice sites, e.g. the half-filled band Hubbard model (Caprara and Rosengren 1997b), the DMRG will converge to a fix point.

It is remarkable that for this case, the DMRG ground state wave function can be written as a matrix product (Östlund and Rommer 1995), which can be derived rigorously through a simple variational ansatz making no reference to the DMRG scheme. Details of this construction are given by Östlund and Rommer (1995). Having at hand the analytic form of the wave function, many properties of the system can be calculated and checked. The most remarkable result is connected to the form of the correlation functions, which

was proven to have *always* an exponential decay (Östlund and Rommer 1995), with the decay constant depending on the number of states kept. That is, in all cases where the DMRG is convergent it inherently predicts exponential decay of correlations functions, and the true behaviour can only be recovered by careful scaling to zero truncation error.

This is not true for fermionic models where the number of fermions is different from the number of sites. As shown by Caprara and Rosengren (1997*b*), the infinite size DMRG in general fails to converge to a fixed point as the size of the system increases, rather it converges to a closed orbit. How close this orbit is will depend on the physical parameters, most importantly on the filling factor. This effect was first observed for the Hubbard model (Caprara and Rosengren 1997*b*) and later on for the Kondo lattice model also (Caprara and Rosengren 1997*a*). A typical example of these fluctuations is depicted in Figs 2 and 3 for the Kondo lattice model. These fluctuations are due to the fact that the electron density in the system necessarily fluctuates, if the system size always increases by two sites each step. This limits the validity of the Östlund and Rommer (1995) rigorous results. It is not even clear if the thermodynamic limit actually resides within the closed

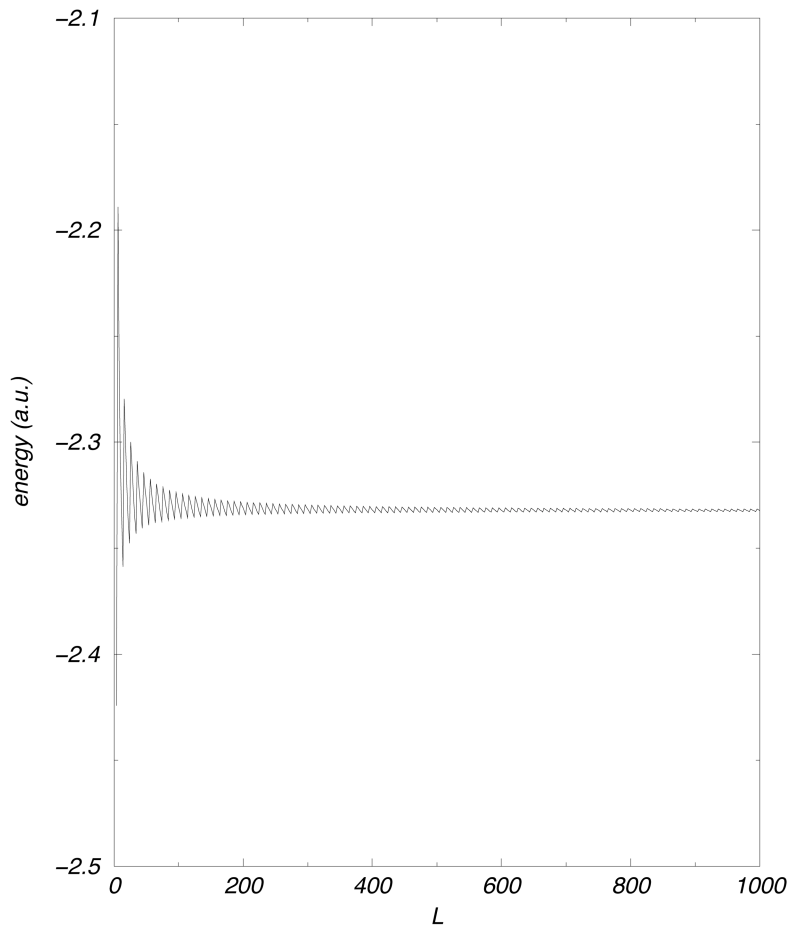


**Fig. 2.** Energy per site as a function of sites  $L$  obtained by using an infinite size DMRG for the Kondo lattice model,  $J = 3.0$  and  $n = 0.9$ . The target state is  $S_{\text{total}} = 0$ .

orbit. The fluctuations in the electron density artificially enhance the electron correlations at that frequency, which can in some cases significantly affect the accuracy of the calculation. It would be possible to avoid the density fluctuations by choosing a different sized environment block such that the lattice size is always an exact multiple of the periodicity of the filling pattern. As far as we know, this variation on the infinite size algorithm has not yet been tried. The extremely good convergence properties of the finite size algorithm mean that this is usually the algorithm of choice for DMRG calculations.

Many other extensions of the original White (1992, 1993) algorithm have been introduced in the past several years. The interested reader is encouraged to consult the recent review papers in this field (see e.g. Hallberg 1999).

## 6. Total Spin DMRG

As mentioned earlier, it is only in the special case of particular quantum numbers that the corresponding operator commutes with the density matrix. For many applications it is useful to keep other quantum numbers, for example the total spin. This allows the calculation

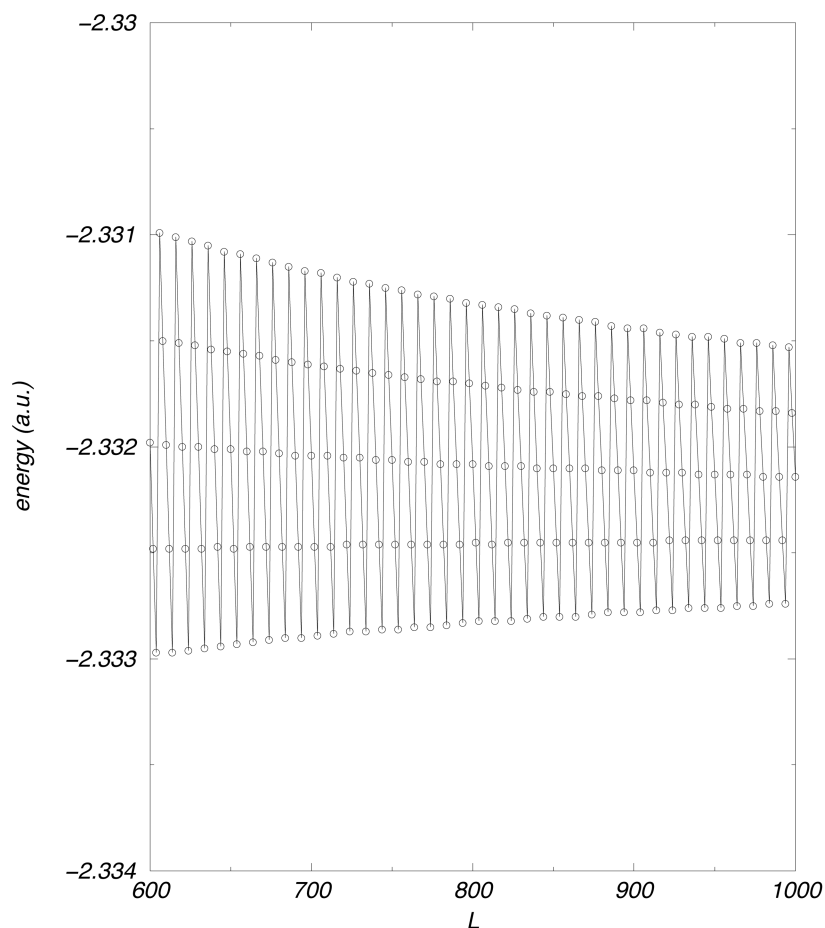


**Fig. 3.** The same as Fig. 2, showing the detailed fluctuations for  $L > 600$ . The circles are the numerical data, while the line is a guide for the eye.



of additional physical quantities, e.g. the energy as a function of magnetisation, which would be difficult without total spin. To this end, we re-formulate the construction of the density matrix, but this time with extra constraints so that we conserve total spin.

Suppose the basis is partitioned into states of total spin, with the basis vectors written as

$$|S, i\rangle, \quad i = 1, 2, \dots, n_S. \quad (6)$$

With this basis the superblock wavefunction has the form

$$|\Psi\rangle = \sum_{\substack{i,j \\ S_1, S_2}} \psi_{S_1, i; S_2, j} |S_1, i\rangle |S_2, j\rangle. \quad (7)$$

Assuming that the wavefunction is an eigenstate of the superblock total spin, the coefficients  $\psi_{S_1, i; S_2, j}$  will not be completely independent, but will be related by the Clebsch–Gordan coefficients. As before we can calculate the weight of an arbitrary block basis state:

$$W(|x\rangle) = \sum_{\substack{i, i', j \\ S_1, S'_1, S_2}} \psi_{S_1, i; S_2, j} \psi_{S'_1, i'; S_2, j}^* \langle x | S_1, i \rangle \langle S'_1, i' | x \rangle, \quad (8)$$

but now we assume that  $|x\rangle$  is an eigenstate of total spin with eigenvalue  $S$ , so that  $\langle x | \mathbf{S}^2 | x \rangle = S^2$ . Maximising the weight gives the desired states, again as an eigenvalue equation

$$\lambda |x\rangle = P |x\rangle, \quad (9)$$

where  $P$  is the *quasi density matrix*,

$$P = \sum_{\substack{i, i', j \\ S_1, S_2}} \psi_{S_1, i; S_2, j} \psi_{S_1, i'; S_2, j}^* |S_1, i\rangle \langle S_1, i'|. \quad (10)$$

The quasi-density matrix is diagonal with respect to the block total spin, and is derived from the ordinary reduced density matrix by neglecting the matrix elements that would mix the total spin states. It is a surprising result that such a simple procedure gives the best possible states, given the total spin constraint. We have not used any properties particular to total spin here, and thus the result holds for arbitrary operator constraints.

The general procedure for applying total spin to the DMRG is shown in Fig. 4. The Clebsch–Gordan transformation requires several different  $z$ -component states for each total spin state. If the quasi-density matrix is calculated independently for each different  $z$ -spin state then the  $S^+$  and  $S^-$  operators will be non-trivial and worse, states needed to represent  $S^+$  and  $S^-$  exactly will be truncated away. While in principle it would be possible to apply the Clebsch–Gordan transformation in this case, the final basis would contain only approximate total spin states, in some circumstances very poor approximations. The computational effort of applying the basis transform would also most likely be prohibitive. Instead, in our scheme we trace over the  $S^z$  values so that the quasi-density matrix is labelled by *multiplets*, rather than individual states. This is equivalent to applying another

1. Add a site to each block,  $A' < A + \text{site}$ ,  $B' < B + \text{site}$
2. Apply the Clebsch-Gordan basis transformation to construct a total spin basis for blocks  $A'$  and  $B'$
3. Construct the superblock from the tensor product of  $A'$  and  $B'$ , targetting as many of the quantum numbers as possible
4. Apply the Clebsch-Gordan transformation to the remaining superblock states, and project onto the target total spin state
5. Diagonalize the superblock and obtain the ground state
6. Invert the Clebsch-Gordan transformation for the ground state to write it as a product of  $A'$  and  $B'$  states
7. Construct the quasi density matrix for block  $A'$
8. Diagonalize the quasi density matrix, keeping the  $m$  spin multiplets of highest weight. This becomes the new block  $A$
9. Return to step 1. as required

**Fig. 4.** The basic algorithm for the DMRG with total spin.

constraint to the weight equation (8) to find the block total spin multiplets of highest weight in the superblock wavefunction, and means that the quasi-density matrix commutes with  $S^+$  as well as  $S^2$ . For systems with  $SU(2)$  symmetry, this is reflected in the matrix elements of the Hamiltonian being independent of the  $z$ -spin state. This can be used to reduce the storage requirement for the block operators. It is best to choose the maximum possible  $z$  spin state ( $S^z = S$ ), as this gives the least number of terms in the Glebsch–Gordan transformation.

For the singlet sector, there is a big efficiency gain. Fig. 5 shows the CPU time per iteration, as a function of the truncation error for the Kondo lattice with total spin 0 versus the  $z$ -spin 0 sector. We have used a 24 site lattice at quarter filling with  $J = 1.0$ , which is in the paramagnetic region with a singlet ground state. With total spin, the speed of the program for  $m$  multiplets is roughly the same as for the conventional DMRG with  $m$  individual states, see Fig. 6. The difference is the overhead of the Clebsch–Gordan transformation—the number of superblock states is identical. Thus effectively we are keeping a factor of  $2s + 1$  more block states (where  $s$  is the average spin of the system block) for the same size superblock. The origin of this huge speed increase is that the  $z$ -spin 0 sector contains every possible integer total spin state, of which the singlet sector is a small subset. In addition, since the singlet state can only be formed out of products of two states with the same total spin, the reduced density matrix contains no elements which are off diagonal with respect to the block total spin, and thus it coincides with the quasi-density matrix. This can be seen in the conventional DMRG, where for a singlet ground state each density matrix eigenvalue is  $(2s + 1)$ -fold degenerate. For higher spin the advantages of keeping the total spin are reduced. For maximum spin, the total spin Hilbert

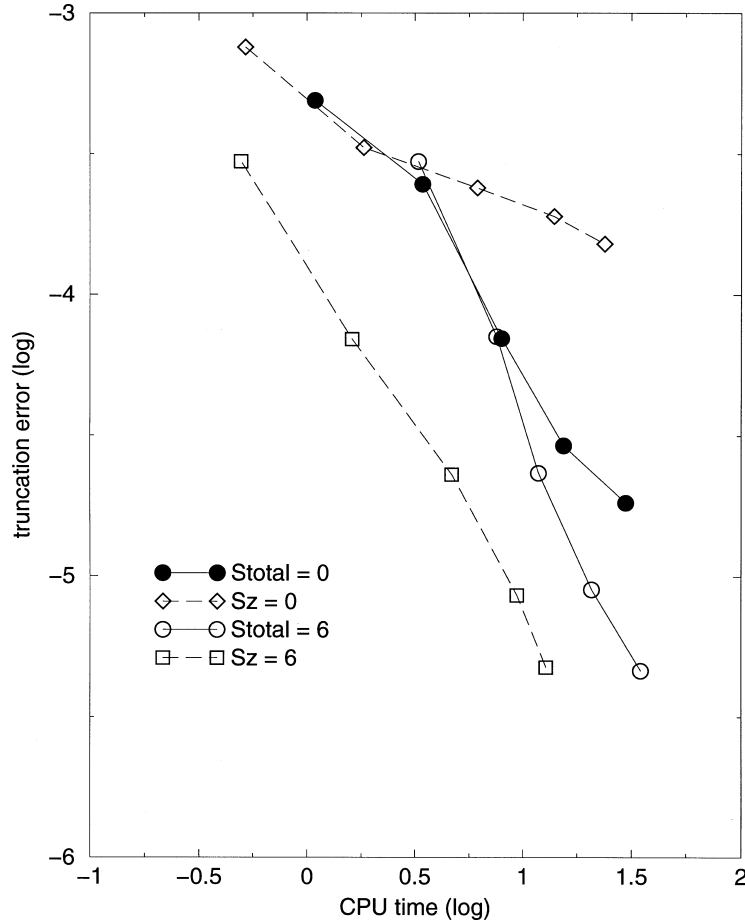


**Fig. 5.** Truncation error versus CPU time, for spin 0 and spin 6, with and without total spin. The data are a finite size DMRG for a 24 site Kondo lattice with  $J = 1.0$  at quarter filling.

space coincides with that given by the  $z$ -spin only, and thus the two algorithms become equivalent at this point (i.e. the Clebsch–Gordan coefficients are unity and again the reduced density matrix contains no elements which are off-diagonal with respect to the block total spin).

For intermediate total spin, it is necessary to further modify the DMRG algorithm to achieve the expected performance gains from total spin. For the Kondo lattice model with intermediate total spin, it is actually necessary to keep  $m$  multiplets to maintain the accuracy of the conventional DMRG with  $m$  states. That is, of the  $2s + 1$  states in each multiplet, there is effectively only one that has appreciable weight in the superblock wavefunction. Moreover, away from the singlet sector keeping  $m$  multiplets in total spin DMRG leads to a bigger superblock than keeping  $m$  states in the conventional DMRG. This is because each system total spin state can combine with several environment block total spin states, within the usual bounds  $|S_1 - S_2| \leq S \leq S_1 + S_2$ , for system total spin  $S_1$ , environment total spin  $S_2$  and superblock total spin  $S$ . Thus each density matrix eigenstate ends up as an average over several sectors of the product Hilbert space, with not

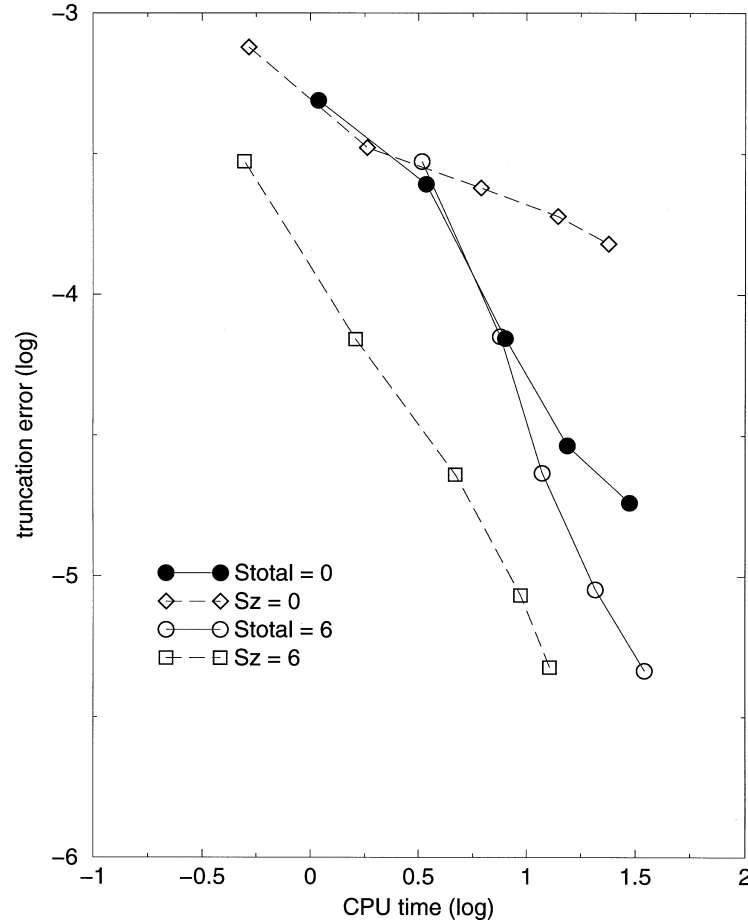


**Fig. 6.** Truncation error versus number of states kept, for spin 0 and spin 6, with and without total spin. The data were obtained in the same conditions as for Fig. 5.

particularly good overlap with any of them. This results in the naive total spin algorithm for intermediate spin performing slower than conventional DMRG. The solution is to again modify the construction of the density matrix so that a different set of basis vectors is kept for each combination of system and environment block spins. This complicates the algorithm because these sets of basis vectors are not orthogonal. The details as to how to implement this will be described in a future publication (McCulloch and Gulácsi 2000).

Fig. 7 shows a comparison of results for the Kondo lattice with 24 sites, at quarter filling with  $J = 1.0$ , which is in the paramagnetic region. The five points correspond to keeping 20, 30, 40, 50 and 60 block states. This shows that even for a small number of states kept, the total spin algorithm gives very good results for the singlet states. With only 60 multiplets kept, the truncation error is  $1.8 \times 10^{-5}$ , an order of magnitude better than 60 states with no total spin. The energy is much lower for a given truncation error. This reflects the fact that a much higher proportion of the Hilbert space contains useful states. Total running time was 1194 seconds with total spin, and 991 seconds without total spin, on a Digital Personal Workstation 500au.

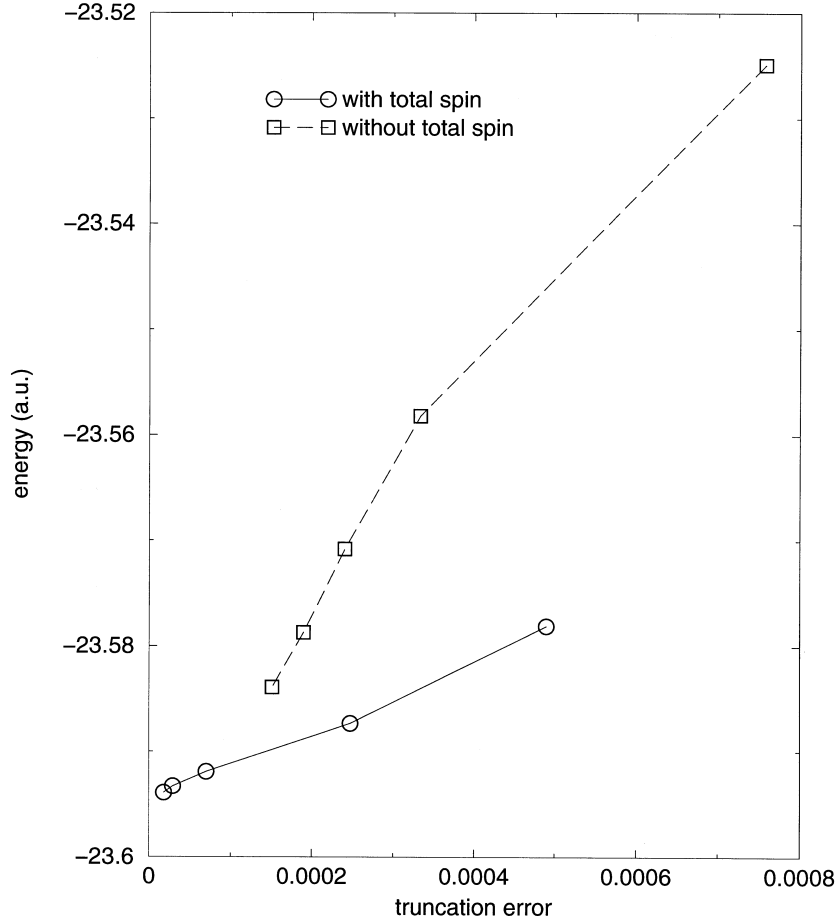


**Fig. 7.** Total energy versus truncation error with and without total spin, for the paramagnetic Kondo lattice—for details see text.

The difference in time corresponds to the overhead of calculating the Clebsch–Gordan transformation, and further optimisation of this section of our codes is possible. In Fig. 8 the results for the Kondo lattice at  $J = 1.6$  are presented. This point is just inside the ferromagnetic region, which has total spin 6. For the case of no total spin, we show both  $S^z = 0$  and  $S^z = 6$  cases. In this case, there are approximately twice as many superblock states when we use total spin, and the computer time with total spin was just under three times that used for no total spin. Thus the results Fig. 8 are not directly comparable with respect to computational time. However, it shows that the energies are again lower for a given truncation error, and the standard error in the curve fit is improved with the limiting energy being  $-27.1704 \pm 0.0001$  without total spin, versus  $-27.17049 \pm 0.00006$  with total spin. The  $S^z = 0$  results are significantly worse than both  $S^z = 6$  and total spin 6.

## 7. Conclusions

In conclusion we have presented an overview of a total spin DMRG and discussed the advantages and disadvantages of using this new algorithm. All the examples presented are

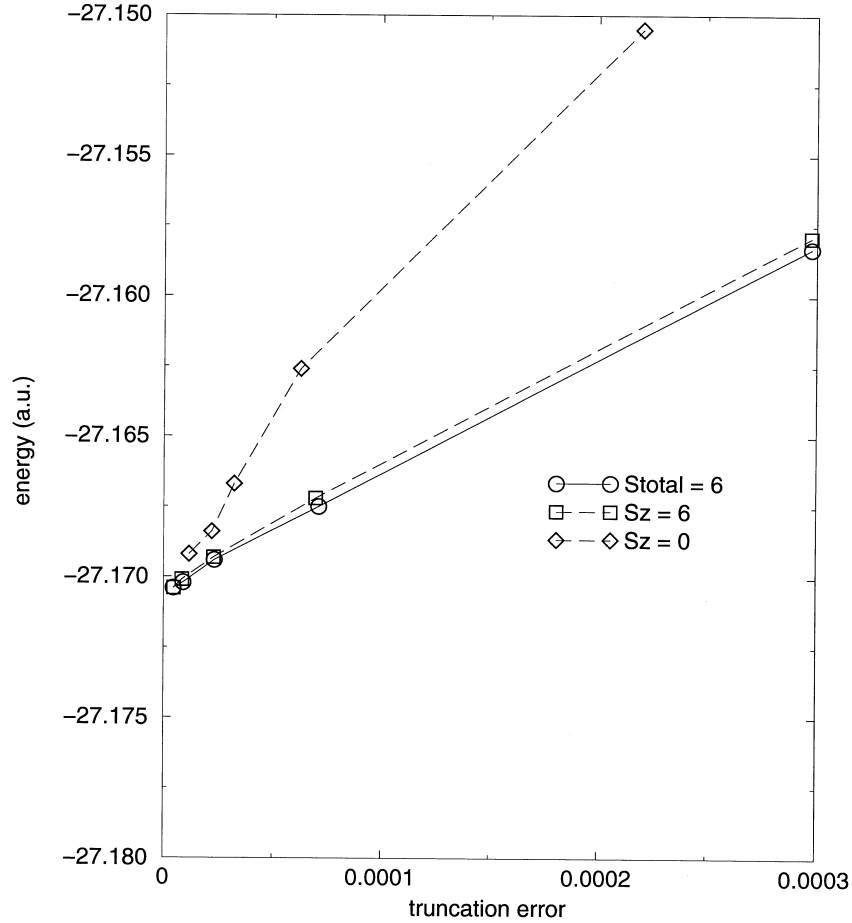


**Fig. 8.** Total energy versus truncation error with and without total spin, for the ferromagnetic Kondo lattice—for details see text.

from the Kondo lattice model. We have chosen this model because it exhibits a large ferromagnetic region, with a peculiar ferromagnetic ordering. One of the issues that we wanted to clarify by using this new program is the controversy over the paramagnetic–ferromagnetic phase boundary close to half filling. Tsunetsugu *et al.* (1997) suggested that ferromagnetism may not appear close to half filling. Previous DMRG algorithms (Troyer and Würtz 1993; Tsunetsugu *et al.* 1993; Moukouri and Caron 1995; Caprara and Rosengren 1997) were unstable for  $n$  greater than quarter filling, because of the oscillations generated by the density—for a discussion see Section 5 above. Our method however, being much more accurate, does not have this problem, and even the infinite size algorithm runs well at fillings of  $n = 0.8, 0.875, 0.9$  and  $0.92$ , where we obtained ferromagnetism (McCulloch *et al.* 1999).

The fluctuations generated by  $n$  are still present in our infinite size algorithm, but they have a minor effect on the convergence. The  $n = 0.9$  case is exemplified in Figs 9 and 10. Both these figures were generated by the infinite size algorithm and show period fluctuations around the density. As can be seen, the magnetisation obtained converges to the

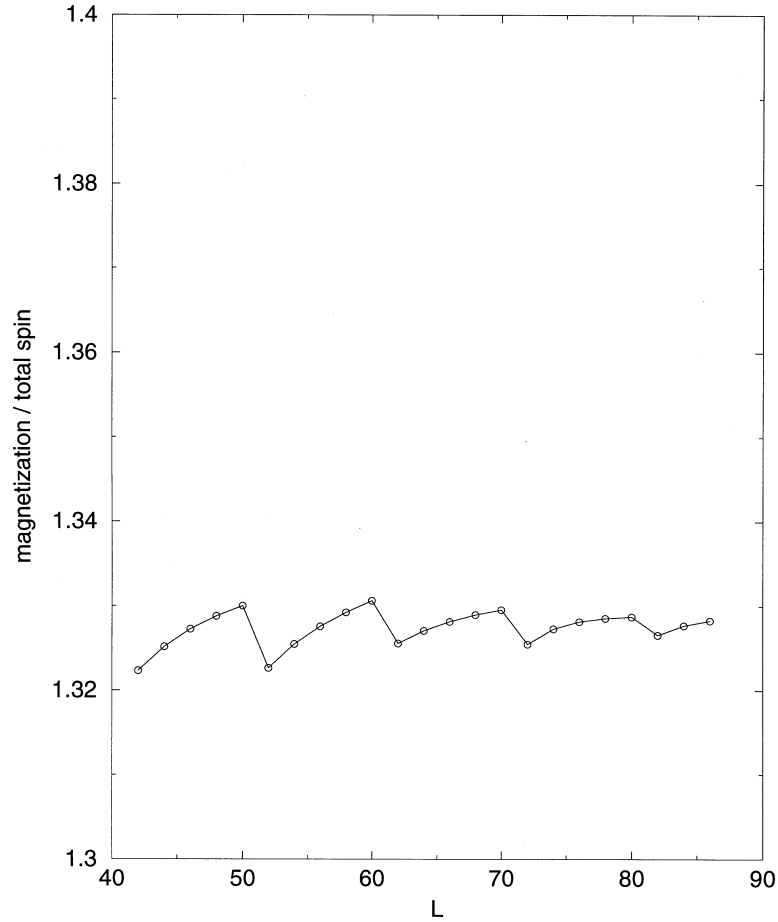


**Fig. 9.** Spontaneous magnetisation per total spin as a function of sites  $L$  obtained by using an infinite size DMRG for the Kondo lattice model,  $J = 3.00$  and  $n = 0.9$ . The circles are the numerical data, while the line is a guide for the eye.

infinite size result as the lattice size is increased. Being such an accurate method, it can be also used to determine the properties of the local ferromagnetic regions, i.e. the ferromagnetic polarons.

The phase transition in this system is different from that in a conventional field theoretical model and does not fit into a typical low-dimensional transition mechanism (Gulácsi and Gulácsi 1998). The behaviour close to the phase transition can be simply understood in terms of ordering of the ferromagnetic polarons. Reducing the Kondo coupling from intermediate values in the ferromagnetic phase, the strong ferromagnetic region is broken up into several large polarons as the system disorders. The remaining clusters occupy a small fraction of the system length but act as if locally they are still in the ordered phase; their magnetisation per unit length is identical to that of the ferromagnetic phase. These remaining rare polarons dominate the low-energy physics in the paramagnetic region.

Accordingly, the flipping of the spin polarons, which determines the quantum dynamics of the model, completely vanishes at the critical line suggesting that the quantum

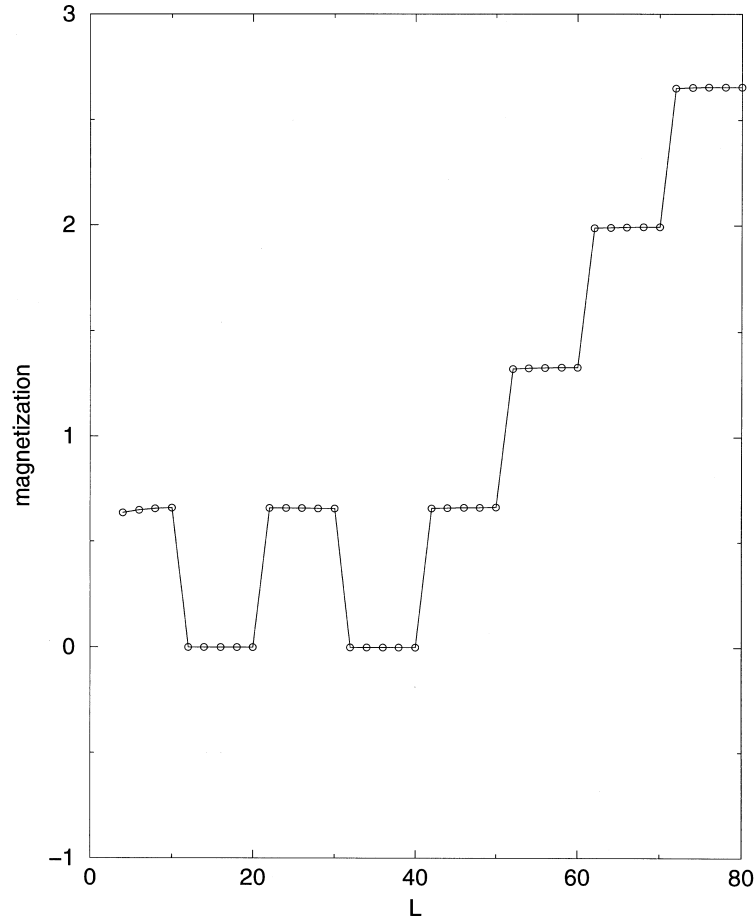


**Fig. 10.** Spontaneous magnetisation as a function of sites  $L$  obtained by using an infinite size DMRG for the Kondo lattice model,  $J = 3.05$  and  $n = 0.9$ . The circles are the numerical data, while the line is a guide for the eye.

fluctuations are asymptotically absent on the critical line, and the model becomes classical at the phase transition (Gulácsi 1999). It would be interesting to see if this type of ordering could also exist in anisotropic antiferromagnets (Gulácsi and McCulloch 1999). For this we will have to extend our study to the periodic Anderson model (Guerrero and Noack 1996), as antiferromagnetism does not appear in the one-dimensional Kondo lattice.

### Acknowledgments

The authors thank S. Caprara, A. Jousapavicius and A. Rosengren for useful discussions. Work in Australia was supported by the Australian Research Council and DISR-IRAP. Work in Sweden was supported by The Göran Gustafsson Foundation, The Carl Trygger Foundation and The Swedish Natural Science Research Council.

### References

- Caprara, S., and Rosengren, A. (1997a). *Europhys. Lett.* **39**, 55.
- Caprara, S., and Rosengren, A. (1997b). *Nucl. Phys. B* **493**, 640.



- Bray, J., and Chui, S. (1987). *Phys. Rev. B* **36**, 8600.
- Guerrero, M., and Noack, R. M. (1996). *Phys. Rev. B* **53**, 3707.
- Gulácsi, M. (1997). *Phil. Mag. B* **76**, 731.
- Gulácsi, M. (1999). In 'Recent Progress in Many-body Theories', Proc. 9th Int. Conf. on Recent Progress in Many-body Theories (Eds D. Neilson and R. F. Bishop), p. 485 (World Scientific: Singapore).
- Gulácsi, M., and McCulloch, I. P. (1999). Group 22, Proc. XII Int. Colloquium on Group Theoretical Methods in Physics (Eds S. P. Corney *et al.*) (International Press: Boston).
- Gulácsi, Zs., and Gulácsi, M. (1998). *Adv. Phys.* **47**, 1.
- Hallberg, K. (1999). cond-mat/9910082.
- Honner, G., and Gulácsi, M. (1997a). *Phys. Rev. Lett.* **78**, 2180.
- Honner, G., and Gulácsi, M. (1997b). *Phil. Mag. B* **76**, 849.
- Honner, G., and Gulácsi, M. (1997c). *Z. Phys. B* **104**, 733.
- Honner, G., and Gulácsi, M. (1998a). *Phys. Rev. B* **58**, 2662.
- Honner, G., and Gulácsi, M. (1998b). *J. Magn. Magn. Mater.* **184**, 307.
- Krishna-murthy, H. R., Wilkins, J. W., and Wilson, K. G. (1980). *Phys. Rev. B* **21**, 1003.
- McCulloch, I. P., and Gulácsi, M. (2000). to be published.
- McCulloch, I. P., Gulácsi, M., Caprara, S., Jouzavavicius, A., and Rosengren, A. (1999). *J. Low Temp. Phys.* **117**, 323.
- Moukouri, S., and Caron, L. G. (1995). *Phys. Rev. B* **52**, R15723.
- Östlund, S., and Rommer, S. (1995). *Phys. Rev. Lett.* **75**, 3537.
- Troyer, M., and Würtz, D. (1993). *Phys. Rev. B* **47**, 2886.
- Tsunetsugu, H., Sigrist, M., and Ueda, K. (1993). *Phys. Rev. B* **47**, 8345.
- Tsunetsugu, H., Sigrist, M., and Ueda, K. (1997). *Rev. Mod. Phys.* **69**, 809.
- Voit, J. (1995). *Rep. Prog. Phys.* **58**, 977.
- White, S. R. (1992). *Phys. Rev. Lett.* **69**, 2863.
- White, S. R. (1993). *Phys. Rev. B* **48**, 10345.
- White, S. R., and Scalapino, D. J. (1997). *Phys. Rev. B* **55**, R14701.
- White, S. R., and Scalapino, D. J. (1998). *Phys. Rev. B* **57**, 3031.
- Wilson, K. G. (1975). *Rev. Mod. Phys.* **47**, 773.